A Tightly-Coupled GNSS/IMU Integration Algorithm for Multi-Purpose INS

A.Y. Shatilov, I.A. Nagin, *NAVIS Inc.*

BIOGRAPHY

Alexander Y. Shatilov is a head of "Integrated Systems Technology" department in NAVIS Inc. since April 2011. He received his Ph.D. (canditate of sciences) in Radar and Radio-Navigation technologies from Moscow Power Engineering Institute, Moscow 2007. His research interests include digital and analog signal processing in GNSS receiver, GNSS/INS integration technologies and CRPA technologies.

Ilya A. Nagin is a research associate in the "Integrated Systems" laboratory, NAVIS Inc. since July 2011. He received his M.S. in Radar and Radio-Navigation technologies from Moscow Power Engineering Institute, Moscow 2007, and now he is Ph.D. candidate. His research interests include digital signal processing in GNSS receiver, GNSS/INS integration and dead reckoning technologies.

ABSTRACT

A tightly-coupled GNSS/INS integration algorithm has been developed. It implements an approach where user dynamics model is expressed via accelerometer and gyro measurements. That resulted in higher computational efficiency and seamless filter design. In proposed algorithm INS data is fed into receiver's tracking loops to compensate line-of-sight dynamics and tighten their bandwidths. It increases the receiver's sensitivity and antijam capability. From the other hand, receiver's PVT (Position, Velocity, Time) output allowed to estimate and compensate IMU errors – that resulted in more precise INS navigation solution in standalone mode (during GNSS outages). The development and simulation results for the proposed algorithm with tactical-grade IMU are presented in this paper.

INTRODUCTION

It is known that the complementary properties of the GNSS (Global Navigation Satellite System) receiver and INS (Inertial Navigation System) allow achieving more accurate, smooth and reliable navigation output when both devices are properly integrated. Tightly-coupled integration scheme assumes that INS data are fed into the tracking loops of the GNSS receiver and it helps compensate for the dynamic component, caused by the user movement. This allows tightening bandwidths of the tracking loops, and hence increasing the sensitivity and antijam capability of the receiver in conditions of high dynamic movement. On the other hand, GNSS output allows estimating and compensating IMU (Inertial Measurement Unit) errors. This compensation leads to a lower growth of INS errors in standalone mode when the GNSS data are not available. Moreover, the compensation of errors of inertial sensors leads to a more accurate aiding of the receiver tracking loops, resulting in even greater gain in sensitivity and antijam capability.

The objectives of the algorithm development are: a) to achieve the maximum antijam capability of the GNSS receiver by using the data from the INS, and b) to reduce the growth of positioning errors during GNSS outages via estimation and compensation of IMU errors when the data from the GNSS are available. The algorithm was considered for use in multi-purpose Inertial-Satellite Navigation System (ISNS) - it does not use any a priori information about the nature of the user movement.

ALGORITHM DEVELOPMENT

We shall carry out the algorithm synthesis within the concept of tightly-coupled integration scheme for the output of the GNSS receiver and outputs of accelerometers and gyroscopes of the IMU.

To achieve high accuracy of navigation solution during the loss of GNSS signal the estimation of the orientation angles, as well as INS coordinates and velocity vector, is required. Besides, it is necessary to estimate not only the errors of navigation parameters themselves, but their root cause – IMU errors. This complicates the algorithm design and adjustment but gives an optimal result in terms of achieving the minimum RMS error of the navigation parameters.

We use IMU measurements model in the form of

$$\mathbf{a}_{rpy,k} = \left(\mathbf{I} + \mathbf{m}_{a,k}\right)\mathbf{A}_{rpy,k} + \mathbf{b}_{a,k} + \mathbf{n}_{a,k},$$
$$\boldsymbol{\omega}_{rpy,k} = \left(\mathbf{I} + \mathbf{m}_{g,k}\right)\boldsymbol{\Omega}_{rpy,k} + \mathbf{b}_{g,k} + \mathbf{n}_{g,k}, \qquad (1)$$

where k is the sample number in IMU's discrete time, $\mathbf{A}_{rpy,k}$ is the true specific force in IMU reference frame (coincident with body frame "Roll-Pitch-Yaw", RPY), $\boldsymbol{\Omega}_{rpy,k}$ is the true absolute angular velocity vector in IMU frame, $\mathbf{b}_{a,k}$, $\mathbf{b}_{g,k}$ are the vectors of accelerometer and gyro biases respectively, $\mathbf{m}_{a,k}, \mathbf{m}_{g,k}$ are the matrices of

the axes misalignment and scale factor errors for accelerometers and gyros, $\mathbf{n}_{a,k}$, $\mathbf{n}_{g,k}$ are the vectors of noise errors, which are assumed to be the white Gaussian noises without cross-correlation. The elements of $\mathbf{m}_{a,k}$, $\mathbf{m}_{g,k}$, $\mathbf{b}_{a,k}$, $\mathbf{b}_{g,k}$ are assumed to be Wiener processes (random walks).

IMU axes of sensitivity are aligned to the physical body axes with some small mounting error, which is fundamentally impossible to eliminate. (In the analysis of inertial algorithms, this error is usually considered to be zero). We take this into account in description of misalignment matrices assuming the "Roll" sensor axis to be strictly coincident with body "Roll" axis. Then misalignment matrices $\mathbf{m}_{a,\omega\equiv x}$ will look like:

$$\mathbf{m}_x = \begin{vmatrix} m_x 11 & 0 & 0 \\ m_x 21 & m_x 22 & m_x 23 \\ m_x 31 & m_x 32 & m_x 33 \end{vmatrix}. \qquad (2)$$

This forced assumption is principal for eliminating the ambiguity of attitude determination.

The measurements model for GNSS receiver include user velocity and position vectors in ECEF frame:

$$\mathbf{X}_{gnss,i} = \mathbf{X}_{ecef,i} + \boldsymbol{\delta}_{X,i},$$
$$\mathbf{V}_{gnss,i} = \mathbf{V}_{ecef,i} + \mathbf{n}_{V,i}, \qquad (3)$$

where i is the sample number in receiver's discrete time, $\mathbf{X}_{ecef,i}$ is the true user coordinates' vector, $\boldsymbol{\delta}_{X,i}$ is the position errors vector with the covariance matrix $\mathbf{R}_{X,i}$; $\mathbf{V}_{ecef,i}$ is the true user velocity vector, $\mathbf{n}_{V,i}$ is the vector of white Gaussian noises with the covariance matrix $\mathbf{R}_{V,i}$; $\mathbf{R}_{X,i}$ and $\mathbf{R}_{V,i}$ are assumed to be known from the navigation solution routine of GNSS receiver.

Measurements from the IMU come with far greater rate than the measurements from the GNSS receiver, as it is shown in figure 1. This is taken into account in the algorithm. In simulation, we assume that the measurements from the gyros and accelerometers come with a rate of 1000 Hz, and measurements from the GNSS receiver come with a typical rate of 10 Hz.

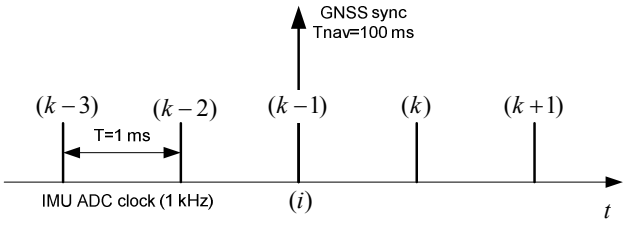

Figure 1. Time alignment for GNSS and IMU measurements

To estimate and compensate IMU errors as well as produce integrated estimates for the velocity, acceleration and orientation vectors we synthesize an integration filter based on the extended Kalman filter (EKF). The main objective for this EKF is to estimate IMU errors $\mathbf{b}_a$, $\mathbf{b}_g$, $\mathbf{m}_a$, $\mathbf{m}_g$. Their subsequent compensation will result in more accurate standalone solution. The only way to estimate these errors is to utilize an additional data source - the GNSS receiver. The receiver provides measurements of the user coordinates and velocities, which may be included in the state vector. In common sense, the measurements of the coordinates are redundant, since all the data about the user dynamic movement is already laid in the velocity vector. Therefore, the user coordinates can be excluded from the EKF state vector - they can be estimated in a separate block. Also, it is necessary to include user attitude parameters (that reflects mutual orientation of IMU RPY frame and the ECEF frame) in the state vector. The complete EKF state vector is represented as follows:

$$\mathbf{x} = \left| \left(\mathbf{V}_{ecef}\right)^{\mathrm{T}} \quad \left(\mathbf{q}_{rpy}^{ecef}\right)^{\mathrm{T}} \quad \left(\mathbf{b}_g\right)^{\mathrm{T}} \quad \left(\vec{\mathbf{m}}_g\right)^{\mathrm{T}} \quad \left(\mathbf{b}_a\right)^{\mathrm{T}} \quad \left(\vec{\mathbf{m}}_a\right)^{\mathrm{T}} \right|^{\mathrm{T}}, \qquad (4)$$

where $\mathbf{q}_{rpy}^{ecef}$ is the quaternion representing the orientation of RPY frame within the ECEF frame; $\vec{\mathbf{m}}_g$ are $\mathbf{m}_g$ matrix elements vectorized rowwise. The total number of elements in state vector $\mathbf{x}$ is 27.

A distinctive feature of the approach used in EKF synthesis is that the dynamic equations for evolution of $\mathbf{q}_{rpy}^{ecef}$ and $\mathbf{V}_{ecef}$ components were written through accelerometers and gyros' measurements. Actually, it led to the fact that the step of Kalman filter extrapolation implements the step of inertial navigation algorithm. The dynamics of $\mathbf{q}_{rpy}^{ecef}$ quaternion can be represented in a discrete-time form as [1]

$$\mathbf{q}_{rpy,k}^{ecef} = \boldsymbol{\Delta}_E^* \otimes \mathbf{q}_{rpy,k-1}^{ecef} \otimes \boldsymbol{\Delta}_{RPY,k}, \qquad (5)$$

where $\otimes$ is the operation of quaternion multiplication; $\boldsymbol{\Delta}_E^*$ is the conjugate quaternion representing small rotation of Earth during $t_{k-1}\ldots t_k$ interval; $\boldsymbol{\Delta}_{RPY,k}$ is the quaternion of user rotation in inertial space during $t_{k-1}\ldots t_k$ interval.

$$\boldsymbol{\Delta}_E^* = \left|\cos\left(\omega_E T/2\right) \quad 0 \quad 0 \quad -\sin\left(\omega_E T/2\right)\right|^{\mathrm{T}}, \qquad (6)$$

ω_E = 7.292115E-5 rad/s – Earth's rotation rate.

$$\boldsymbol{\Delta}_{RPY,k} = \mathbf{Q}\left(\boldsymbol{\rho}_k\right),\ \boldsymbol{\rho}_k \approx \frac{T}{2}\left(\boldsymbol{\Omega}_{rpy,k} + \boldsymbol{\Omega}_{rpy,k-1}\right), \qquad (7)$$

where $\mathbf{Q}\left(\boldsymbol{\rho}_k\right)$ is the function that transforms rotation vector $\boldsymbol{\rho}_k$ to the quaternion [1,2].

With the help of gyroscope measurement model (1) $\boldsymbol{\Omega}_{rpy}$ can be expressed in (7) through the measurements $\boldsymbol{\omega}_{rpy,k}$ and their errors:

$$\boldsymbol{\Omega}_{rpy,k} = \left(\mathbf{I} + \mathbf{m}_{g,k}\right)^{-1}\left(\boldsymbol{\omega}_{rpy,k} - \mathbf{b}_{g,k} - \mathbf{n}_{g,k}\right),$$
$$\boldsymbol{\rho}_k \approx T \cdot \left(\mathbf{I} - \mathbf{m}_{g,k-1}\right)\left[\frac{1}{2}\left(\boldsymbol{\omega}_{rpy,k} + \boldsymbol{\omega}_{rpy,k-1}\right) - \mathbf{b}_{g,k-1}\right] + \mathbf{n}_{\rho,k}, \qquad (8)$$

where $\mathbf{n}_{\rho,k} \approx -\frac{T}{2}\left(\mathbf{n}_{g,k} + \mathbf{n}_{g,k-1}\right)$. The expressions for $\boldsymbol{\rho}_k$ in (8) are obtained under the assumption that $\mathbf{m}_{g,k} \approx \mathbf{m}_{g,k-1}$, $\mathbf{b}_{g,k} \approx \mathbf{b}_{g,k-1}$, $\left(\mathbf{I}+\mathbf{m}_g\right)^{-1} \approx \left(\mathbf{I}-\mathbf{m}_g\right)$. Vector of noise $\mathbf{n}_{\rho,k}$ can be neglected for all types of gyroscopes (FOG, RLG, mechanical), except for the micromechanical (MEMS) ones. The expressions (5) - (8) represent the dynamic model for $\mathbf{q}_{rpy}^{ecef}$. They also determine the attitude reckoning algorithm in a strapdown INS.

The dynamic model for $\mathbf{V}_{ecef}$ follows from the general navigation equation [2]

$$\frac{\mathrm{d}\mathbf{V}_{ecef}(t)}{\mathrm{d}t} = \mathbf{C}\left(\mathbf{q}_{rpy}^{ecef}(t)\right)\cdot\mathbf{A}_{rpy}(t) - 2\boldsymbol{\Omega}_{EX}\mathbf{V}_{ecef}(t) + \mathbf{g}\left(\mathbf{X}_{ecef}(t)\right), \tag{9}$$

where $\mathbf{A}_{rpy}(t)$ is the specific force in RPY frame; $\mathbf{C}\left(\mathbf{q}_{rpy}^{ecef}(t)\right)$ is the transition matrix from the RPY to the ECEF, expressed through the components of the quaternion $\mathbf{q}_{rpy}^{ecef}$ [1]; $\mathbf{g}\left(\mathbf{X}_{ecef}(t)\right)$ is the gravitational acceleration in ECEF (includes the centripetal acceleration due to the Earth rotation);

$$\boldsymbol{\Omega}_{EX} = \begin{vmatrix} 0 & -\omega_E & 0 \\ \omega_E & 0 & 0 \\ 0 & 0 & 0 \end{vmatrix}.$$

Having performed a discrete numerical integration of eq. (9) with $\mathbf{A}_{rpy,k} = \left(\mathbf{I}-\mathbf{m}_{a,k}\right)\left(\mathbf{a}_{rpy,k} - \mathbf{b}_{a,k} - \mathbf{n}_{a,k}\right)$ (from (1)) we can get a dynamic model of $\mathbf{V}_{ecef}$ for EKF synthesis in the form:

$$\begin{aligned}
&\mathbf{V}_{ecef,k} = \left(\mathbf{I} - 2T\boldsymbol{\Omega}_{EX}\right)\mathbf{V}_{ecef,k-1} + \mathbf{g}\left(\bar{\mathbf{X}}_{ecef,k}\right)T + \\
&\quad + \frac{T}{2}\left[\mathbf{C}\left(\mathbf{q}_{rpy,k}^{ecef}\right)\cdot\tilde{\mathbf{A}}_{rpy,k} + \mathbf{C}\left(\mathbf{q}_{rpy,k-1}^{ecef}\right)\cdot\tilde{\mathbf{A}}_{rpy,k-1}\right] + \mathbf{n}_{DV,k}, \\
&\tilde{\mathbf{A}}_{rpy,k} = \left(\mathbf{I}-\mathbf{m}_{a,k-1}\right)\left(\mathbf{a}_{rpy,k} - \mathbf{b}_{a,k-1}\right), \\
&\tilde{\mathbf{A}}_{rpy,k-1} = \left(\mathbf{I}-\mathbf{m}_{a,k-1}\right)\left(\mathbf{a}_{rpy,k-1} - \mathbf{b}_{a,k-1}\right),
\end{aligned} \tag{10}$$

where $\tilde{\mathbf{A}}_{rpy,k}$, $\tilde{\mathbf{A}}_{rpy,k-1}$ are the compensated measurements of the accelerometers; $\mathbf{n}_{DV,k}$ is the vector of noise, reflecting the sum of model inaccuracy with the noise of the accelerometers. $\mathbf{n}_{DV,k}$ is assumed to be white Gaussian noise with non-stationary covariance matrix $\mathbf{D}_{DV,k}$. The elements of $\mathbf{D}_{DV,k}$ matrix are very small, and in some cases they can be considered as zeros.

Gravity vector $\mathbf{g}\left(\bar{\mathbf{X}}_{ecef,k}\right)$ is approximated by the known functionality [3]. The $\bar{\mathbf{X}}_{ecef,k}$ estimates are formed in special way to eliminate the effect of INS' vertical channel instability.

EKF implementation consists of the following steps.

1. Initialization of the state vector and its covariance matrix.

$$\hat{\mathbf{x}}_0 = \left|\left(\mathbf{V}_{gnss,i}\right)^{\mathrm{T}} \quad \left(\mathbf{q}_{rpy}^{ecef}\left(R_0, P_0, Y_0\right)\right)^{\mathrm{T}} \quad 0\ldots0\right|^{\mathrm{T}}, \tag{11}$$

where $\mathbf{V}_{gnss,i}$ is the current velocity vector measured by the GNSS receiver, $\mathbf{q}_{rpy}^{ecef}\left(R_0, P_0, Y_0\right)$ is the attitude quaternion which can be obtained as a result of initial INS alignment (gyrocompassing) procedure. The initial value for state vector covariance matrix $\mathbf{E}_0$ is set in accordance with initial uncertainties of the state vector elements.

2. Prediction of the state vector.
The predicted estimate of the state vector can be written in general form as: $\tilde{\mathbf{x}}_k = \mathbf{f}\left(\hat{\mathbf{x}}_{k-1}\right)$, where $\mathbf{f}(\,)$ is a known functionality defined by the dynamic model which includes eq. (5)-(8), (10). We denote the a-posteriori estimate of any parameter with "^" symbol and the predicted estimate of this parameter with "~" symbol. In particular, the $\mathbf{V}_{ecef}$ subvector is predicted in accordance with eq. (10), the $\mathbf{q}_{rpy}^{ecef}$ subvector - in accordance with eq. (5)-(8), and other components - in accordance with the dynamic model of random walk.

3. Prediction of the covariance matrix.
The dynamic model of the EKF state vector can be written in the form of a Markov process

$$\mathbf{x}_k = \mathbf{f}\left(\mathbf{x}_{k-1}\right) + \mathbf{G}\left(\mathbf{x}_{k-1}\right)\cdot\boldsymbol{\xi}_k, \tag{12}$$

where $\boldsymbol{\xi}_k$ is the vector of discrete white Gaussian noises with identity covariance matrix. Therefore the EKF covariance matrix is predicted as

$$\tilde{\mathbf{E}}_k = \frac{\partial\mathbf{f}\left(\hat{\mathbf{x}}_{k-1}\right)}{\partial\mathbf{x}_{k-1}}\mathbf{E}_{k-1}\left(\frac{\partial\mathbf{f}\left(\hat{\mathbf{x}}_{k-1}\right)}{\partial\mathbf{x}_{k-1}}\right)^{\mathrm{T}} + \mathbf{P}, \tag{13}$$

where $\mathbf{P} \equiv \mathbf{G}\left(\tilde{\mathbf{x}}_k\right)\cdot\mathbf{G}\left(\tilde{\mathbf{x}}_k\right)^{\mathrm{T}}$ - a constant matrix in our case.

4. Estimation.
If the reliable measurements ($\mathbf{V}_{gnss,k}$, $\mathbf{X}_{gnss,k}$) from the GNSS receiver are available, the EKF estimation step is performed. It can be described by the equations

$$\begin{aligned}
&\mathbf{K}_k = \tilde{\mathbf{E}}_k\cdot\mathbf{H}^{\mathrm{T}}\cdot\left(\mathbf{H}\cdot\tilde{\mathbf{E}}_k\cdot\mathbf{H}^{\mathrm{T}} + \mathbf{R}_{V,k}\right)^{-1}, \\
&\mathbf{E}_k = \left(\mathbf{I} - \mathbf{K}_k\cdot\mathbf{H}\right)\cdot\tilde{\mathbf{E}}_k, \\
&\hat{\mathbf{x}}_k = \tilde{\mathbf{x}}_k + \mathbf{K}_k\cdot\left(\mathbf{V}_{gnss,k} - \tilde{\mathbf{V}}_{ecef,k}\right),
\end{aligned} \tag{14}$$

where $\mathbf{H} = \left|\mathbf{I}_3 \quad \mathbf{0}_{3\times24}\right|$, $\mathbf{K}_k$ is the matrix of EKF coefficients.

Note that heavy operation of matrix inversion in (14) is performed only in sparse moments of GNSS measurements availability. Moreover, the matrix to

inverse have only 3x3 dimension and could be inverted analytically. Therefore, despite the large EKF size (27 states), it is very effective computationally.

GNSS measurements are taken into account only at the EKF estimation step. At this very moment the estimation of IMU sensor errors takes place as well. In the absence of reliable measurements from the GNSS receiver there is no EKF estimation steps, and EKF is operating in the prediction mode only:

$$\hat{\mathbf{x}}_k = \tilde{\mathbf{x}}_k\,, \qquad \mathbf{E}_k = \tilde{\mathbf{E}}_k\,. \tag{15}$$

EKF prediction step is nothing but the algorithm of reckoning in standalone INS. Therefore, the transition from the integrated mode to the standalone reckoning mode in the proposed ISNS is performed seamlessly and transparently.

The estimation of coordinates together with the integrity monitoring of GNSS measurements is implemented in a separate block. Estimation of the coordinates is performed by the simple initialization of INS position from the GNSS position. Integrity monitoring is based on the analysis of the position and velocity measurements from GNSS and their comparison with the predicted estimates of these parameters from integration filter. We shall not consider this part of the tightly-coupled algorithm because it is out of scope of this paper.

EKF, the position estimation block and the integrity monitoring block construct an integration filter for system's secondary data processing unit. The structure of this unit is shown in fig. 2.

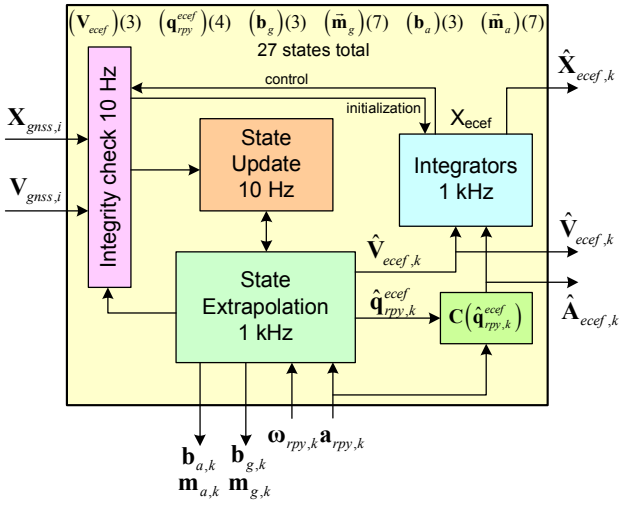

Figure 2. Integration filter internals

The user acceleration in ECEF is evaluated from the compensated accelerometer outputs with the use of the velocity and attitude estimates from EKF:

$$\hat{\mathbf{A}}_{ecef,k} = \mathbf{C}\left(\tilde{\mathbf{q}}^{ecef}_{rpy,k}\right)\cdot\tilde{\mathbf{A}}_{rpy,k} - 2\boldsymbol{\Omega}_{EX}\tilde{\mathbf{V}}_{ecef,k} + \mathbf{g}\left(\hat{\mathbf{X}}_{ecef,k}\right), \tag{16}$$

where $\tilde{\mathbf{A}}_{rpy,k}$ is calculated according to eq. (10).

Acceleration vector $\hat{\mathbf{A}}_{ecef,k}$ is used to calculate the line-of-sight (LOS) accelerations to aid the GNSS receiver tracking loops. The LOS acceleration is the second derivative of the distance between the satellite and the user. The algorithm for LOS accelerations calculation is given below.

$$\mathbf{R}_k = \frac{(\hat{\mathbf{X}}_{ecef,k} - \mathbf{X}_{sat,k})}{D_k}\,,\ D_k = \left\|\hat{\mathbf{X}}_{ecef,k} - \mathbf{X}_{sat,k}\right\|, \tag{17}$$

$$Vaid_k = (\hat{\mathbf{V}}_{ecef,k} - \mathbf{V}_{sat,k})^{\mathrm{T}}\cdot\mathbf{R}_k\,, \tag{18}$$

$$Aaid_k = \left(\hat{\mathbf{A}}_{ecef,k} - \mathbf{a}_{sat,k}\right)^{\mathrm{T}}\cdot\mathbf{R}_k - \frac{\left\|\hat{\mathbf{V}}_{ecef,k} - \mathbf{V}_{sat,k}\right\|^2}{D_k} + \frac{Vaid_k^2}{D_k}\,, \tag{19}$$

where $\mathbf{X}_{sat,k}$, $\mathbf{V}_{sat,k}$, $\mathbf{a}_{sat,k}$ are the coordinates, velocity and acceleration vectors of the given satellite; $\mathbf{R}_k$ is the vector of the unit length pointing to satellite; D_k is the distance to the given satellite; $Vaid_k$, $Aaid_k$ are the calculated values of LOS velocity and LOS acceleration, respectively. The issues of primary data processing in the GNSS receiver with the aiding of tracking loops by LOS acceleration are widely highlighted in the references [1], [5], [6], [7]. This system applies the well-known methods for tracking loops aiding, on which we are not going to focus.

The block diagram for ISNS implementing the proposed integration algorithm is shown in figure 3.

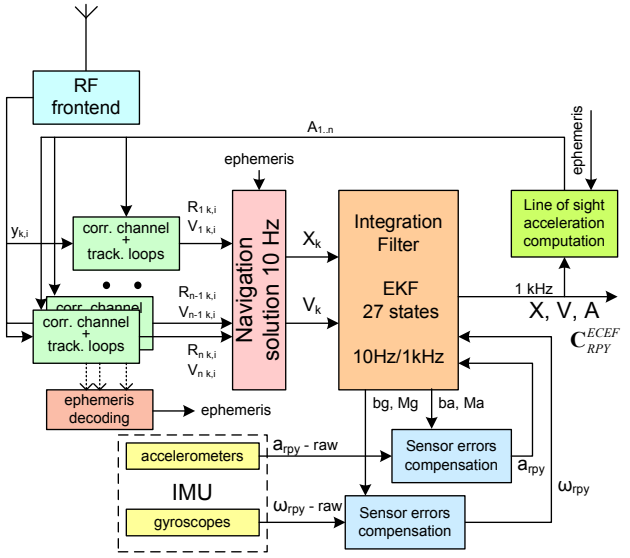

Figure 3. Tightly coupled ISNS design

This scheme is resulted from the tightly-coupled approach. One of its useful advantages is a small number of links between GNSS receiver and INS. It is supposed that main navigation computer (running integration filter software) is placed in INS unit. Such a design simplifies the modernization of existing INSes and it is good for

creating the new ones.

SIMULATION RESULTS

To evaluate the characteristics of precision, convergence and antijam capability of the proposed algorithm the simulation has been carried out. Simulation model included tactical grade IMU with performance characteristics presented in table 1.

Table 1. IMU characteristics

Gyros	
Bias (1σ)	0.1 °/h
Accuracy of scale (1σ)	10^{-4}
Misalignment of measurement axes (1σ)	5 ang. min.
Noise component (1σ)	1.8E-7 rad/s
Accelerometers	
Bias (1σ)	10^{-4} g
Accuracy of scale (1σ)	10^{-4}
Misalignment of measurement axes (1σ)	5 ang. min.
Noise component (1σ)	1.72E-5 m/s^2

Antijam capability of the GNSS receiver was estimated under operation upon new L3OC GLONASS signals with 20.46 MHz bandwidth. L3OC signals are very similar to GPS L5 ones. It's very important that L3OC signal, as well as L5, has pilot component. Only coherent mode was considered. The jammer modeled as a band-limited Gaussian noise with flat spectrum within the L3OC band.

It is known that the dynamics of the reference oscillator drift dramatically affects antijam capability. Oscillator's frequency drift was modeled by random-walk process, according to [6], with the parameter $S_{0\Gamma}$ =11 rad^2/s^3 that roughly corresponds to Allan deviation of 1x10^{-10} at τ = 1 s. For test purposes, the dynamics of user movement was modeled by a sinusoidal acceleration of 50 g (max) and the sinusoidal jerk 50 g/s (max).

The simulation results are shown in table 2. They are related to different modes of ISNS operation:

- integrated mode after EKF settle, that means that initial transient process in EKF is finished and GNSS measurements are always available (normal ISNS operation in the most of time);
- GNSS only mode, that means that only GNSS receiver is considered - no integration or aiding applied;
- INS only mode, that means that no GNSS data available from the startup moment, whereas initial alignment of INS has been done with zero errors;
- standalone mode, that means that GNSS data are not available due to outage, but the initial transient process in EKF is finished before the outage has begun, and IMU sensor errors are being compensated.

Table 2. Simulation results.

Mode	**Integrated mode after EKF settle**	**GNSS only**	**INS only**	**Standalone (during GNSS outage)**
Positioning error (± 2 σ), m	0.15*	0.7*	800 after 10 min	25 after 10 min
Velocity error (± 2 σ), m/s	0.004	0.8	5 after 10 min	0.15 after 10 min
Attitude error (± 2 σ), ang. min.	0.4	N/A	4 after 10 min	0.5 after 10 min
Antijam capability of L3OC signal tracking: (J/S), dB	67…70	50…52	N/A	N/A

* Only noise errors (no multipath, ionosphere, ephemeris etc. errors considered).

The convergence time of EKF is 250-300 seconds. After this time the velocity and attitude errors come to the constant level. This is depicted in figure 4, which shows velocity errors during initial transient process in EKF.

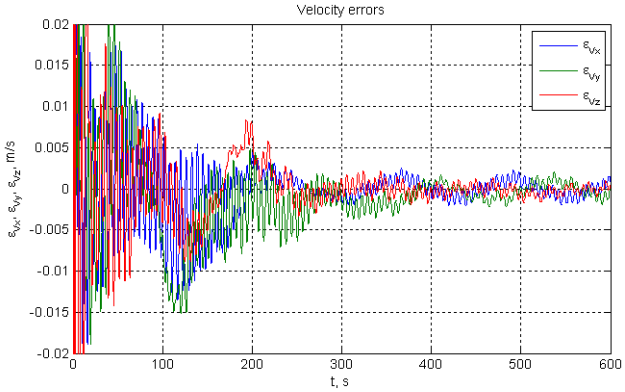

Figure 4. Velocity errors in the integration mode

Antijam capability (J/S) of GNSS L3OC signal tracking mode in the proposed ISNS is 67 ... 70 dB, that is 17 dB higher than the antijam capability of the GNSS receiver without aiding from IMU/integration algorithm.

The simulation showed that the algorithm effectively estimates and compensates IMU sensor errors (biases, scales, and misalignments) by using data from GNSS receiver. This is illustrated in figure 5.

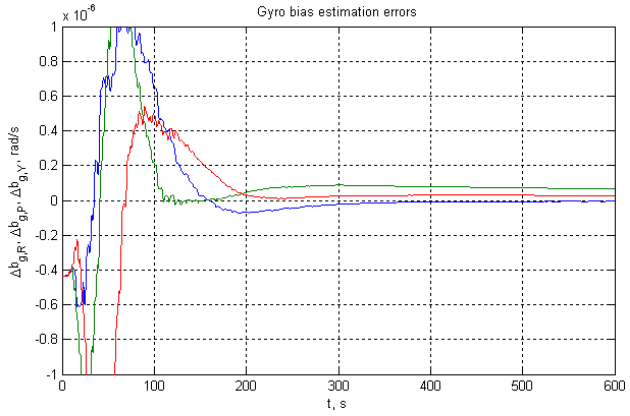

Figure 5. Gyro bias estimation errors

Fig. 5 shows that the gyro bias estimation errors are dramatically reduced (through the transition process) from the initial value of -0.4×10^{-6} rad/s to $\pm 0.05 \times 10^{-6}$ rad/s. It explains why positioning error in standalone mode, where IMU errors are compensated, grows much slower than that in INS only mode, where IMU errors are not compensated.

CONCLUSION

The algorithm is designed to be implemented in the multi-purpose INS consisting of three separate components: GNSS receiver, IMU and the navigation computer. The separation of the algorithm into several parts makes it easier to implement it in a target device. Thus, the algorithm can be used in a large number of integrated GNSS/INS systems for aviation and military applications, as well as in low-cost civil systems based on MEMS sensors.

Note that the algorithm did not use any a priori information specific to the particular user. That is, any inherent dependences, binding the specific forces and angular velocities with the navigation parameters of the object are absent. This ensures that the algorithm does not depend on the specific movement characteristics of the target object.

Integration part of the algorithm is based on the extended Kalman filter, which state vector includes the velocity of the user, the user orientation in quaternion form and IMU sensor errors (27 elements total). A distinctive feature of this EKF is that the user dynamics model is expressed through the measurements of accelerometers and gyroscopes. This leads to the 'seamless' structure of the filter, which implements the inertial navigation algorithm during prediction (extrapolation) step of the EKF. Correction (estimation) step of the filter takes place only when GNSS receiver measurements are available. This approach ensures reliable operation of the algorithm during GNSS outages, a good estimate of EKF covariances and convenient software implementation of the algorithm.

EKF state vector includes the most popular IMU errors: the biases, scale factors and axes misalignments. This allows to use any type of IMU - from the navigation grade IMU to the low-grade MEMS-based one. The changing of IMU type requires only tuning up the constant parameters of the filter.

To avoid the problem of uncertain orientation caused by the mutual misalignment of accelerometers', gyroscopes' and body RPY axes the method of the reference axis is introduced. The method assumes that the one of the accelerometer axis and one of the gyro axis coincide with the corresponding body axis. Thus, the matrices of the axes misalignment are reduced from 9 to 7 elements, which reduces the size of state vector and hence the computational complexity.

The tracking loops aiding part of the algorithm uses the estimate of the acceleration vector in the ECEF frame from the output of the integration filter. Under extremely high user dynamics (max. jerk 50 g/s, max. acceleration 50g) the aiding allows to tighten the PLL bandwidth from 42 Hz to 0.7-1 Hz, which leads to an increase of antijam capability by 17 dB. (Of course, the lower user dynamics the lower will be antijam capability gain).

In general, the simulation results show that the algorithm allows achieving more precise, continuous and reliable navigation solution that is not available for either INS or GNSS receiver alone. This was made possible by the effective estimation and compensation of IMU sensor errors by using the information from the GNSS receiver.

ACKNOWLEDGMENTS

Authors would like to acknowledge the leaders of NAVIS Inc. for financial support of this publication and "NPK Elektrooptika" Ltd. for initiation of this work. Authors are also grateful to prof. Perov A.I. of Moscow Power Engineering Institute for consultations.

REFERENCES

[1] GLONASS. Principles of design and operation / Ed. by Perov A.I., Kharisov V.N. - Moscow: Radiotechnika, 2010.

[2] Salychev O.S., Applied Inertial Navigation: Problems and Solutions. – Moscow, BMSTU Press, 2004.

[3] DEPARTMENT OF DEFENSE WORLD GEODETIC SYSTEM 1984. Its Definition and Relationships with Local Geodetic Systems. - http://earth-info.nga.mil/GandG/publications/tr8350.2/wgs84fin.pdf

[4] Grewal M. S., Weill L.R., Andrews A.P., Global Positioning Systems, Inertial navigation, and Integration. - NewYork: A John Wiley & Sons, Inc. Publication, 2001.

[5] Kaplan Elliott D., Hegarty Christopher J., Understanding GPS: principles and applications.—2nd ed. ARTECH HOUSE, INC., Norwood, MA, 2006.

[6] Shatilov A. Y., The Bandwidth and Antijam Capability of the Integrated PLL/INS.// Radiotechnika. Radiosystemy. №7 2009, Moscow: Radiotechnika 2009, pp. 113-120.

[7] Shatilov A. Y., The Bandwidth and Antijam Capability of the Integrated FLL/INS // Radiotechnika. Radiosystemy. №7 2011, Moscow: Radiotechnika 2011, pp. 87-94.

[8] Shatilov A. Y., The Failure Criteria for Tracking Loop Antijam Capability, Radiotechnika №11 2010, Moscow: Radiotechnika 2010, pp. 29-33.